

Observation of a *d*-wave nodal liquid in highly underdoped $\text{Bi}_2\text{Sr}_2\text{CaCu}_2\text{O}_{8+\delta}$

U. Chatterjee^{1,2}, M. Shi³, D. Ai^{1,2}, J. Zhao^{1,2}, A. Kanigel⁴, S. Rosenkranz², H. Raffy⁵, Z. Z. Li⁵, K. Kadowaki⁶, D. G. Hinks², Z. J. Xu⁷, J. S. Wen⁷, G. Gu⁷, C. T. Lin⁸, H. Claus², M. R. Norman², M. Randeria⁹ and J. C. Campuzano^{1,2,*}

A key question in condensed-matter physics is to understand how high-temperature superconductivity emerges on adding mobile charged carriers to an antiferromagnetic Mott insulator. We address this question using angle-resolved photoemission spectroscopy to probe the electronic excitations of the non-superconducting state that exists between the Mott insulator and the *d*-wave superconductor in $\text{Bi}_2\text{Sr}_2\text{CaCu}_2\text{O}_{8+\delta}$. Despite a temperature-dependent resistivity characteristic of an insulator, the excitations in this intermediate state have a highly anisotropic energy gap that vanishes at four points in momentum space. This nodal-liquid state has the same gap structure as that of the *d*-wave superconductor but no sharp quasiparticle peaks. We observe a smooth evolution of the excitation spectrum, along with the appearance of coherent quasiparticles, as one goes through the insulator-to-superconductor transition as a function of doping. Our results suggest that high-temperature superconductivity emerges when quantum phase coherence is established in a non-superconducting nodal liquid.

High-temperature superconductivity in the cuprates occurs by doping a Mott insulator for which the antiferromagnetic ground state and low-energy excitations are well understood¹. By adding carriers, the parent insulator turns into a superconductor for dopings that exceed 0.05 holes per CuO_2 plane. The *d*-wave nature of the superconducting ground state² and its low-lying excitations are also well understood. Between these phases lies an electronic ground state that is poorly understood. As the temperature is raised, this intermediate ‘pseudogap’ state occupies a larger and larger region of the phase diagram (Fig. 1a). It is from this phase that superconductivity emerges for all but the most highly doped samples. Consequently, the nature of this phase holds the key to the origin of high-temperature superconductivity.

Whereas the electronic excitations in the high-temperature pseudogap region have been studied extensively, there is little spectroscopic data at low temperatures, as there is only a very narrow window of dopings where neither superconducting nor antiferromagnetic order occurs. Here, we present angle-resolved photoemission spectroscopy (ARPES) data on single crystals and thin films³ with doping levels that range all the way from the insulator to the over-doped superconductor. We focus in particular on non-superconducting thin films, just to the left of the superconducting transition temperature T_c dome

(see Fig. 1a), with an estimated hole doping ~ 0.04 (ref. 3). It is normally quite difficult to span the insulator–superconductor transition in $\text{Bi}_2\text{Sr}_2\text{CaCu}_2\text{O}_{8+\delta}$ single crystals. However, it is possible to obtain very underdoped thin films by removing oxygen without film decomposition, as their large surface/volume ratio allows much lower annealing temperatures than those required for crystals. The integrity of the insulating films was confirmed by re-oxygenating them and checking their resistivity $R(T)$ and X-ray diffraction spectra³.

Once sufficient oxygen is removed, the samples have an insulating upturn in resistance $R(T)$ with decreasing temperature, shown in Fig. 1b, that is well described by two-dimensional-variable range hopping^{4,5} (see Supplementary Information). We have measured the diamagnetic susceptibility down to 1.5 K, finding no trace of superconductivity (sensitivity: 1% of volume fraction).

Figure 1d shows the energy distribution curves (EDCs, spectra at constant momentum \mathbf{k} versus binding energy). Despite the low temperature, no sharp, coherent features are discernible in the spectra. This is not surprising, because earlier work had found a strong suppression of coherent spectral weight in the superconducting state with underdoping⁶. In contrast, the momentum distribution curves (MDCs) in Fig. 1e at zero energy show clearly visible peaks. Thus, the excitations are much better defined in \mathbf{k} -space than they are in energy, and are sharper near the zone diagonal than near its boundary (the Brillouin zone is shown in Fig. 1c). Remarkably, despite the insulating-like nature of the resistivity, the MDC peaks indicate a locus of minimum energy excitations similar to that of the superconductors, visible in the ARPES intensity map in Fig. 1c. These ‘Fermi momentum’ (\mathbf{k}_F) values were in fact used to generate the EDCs in Fig. 1d. Figure 1f shows the ARPES intensity as a function of energy and \mathbf{k} for another sample at the same doping, which shows that there is a well-defined dispersion despite the incoherent nature of the EDCs.

To better understand the electronic excitations in the insulator, we plot in Fig. 2d its EDCs at \mathbf{k}_F , symmetrized to remove the effects of the Fermi function⁷, and compare them with superconducting state spectra (Fig. 2e–g) at various dopings indicated in Fig. 2a. In Fig. 2d–g, the top curve corresponds to \mathbf{k}_F on the zone boundary ($\theta = 0^\circ$), whereas the lowest curve corresponds to \mathbf{k}_F on the zone diagonal ($\theta = 45^\circ$), with the Fermi surface angle θ increasing from top to bottom.

¹Department of Physics, University of Illinois at Chicago, Chicago, Illinois 60607, USA, ²Materials Science Division, Argonne National Laboratory, Argonne, Illinois 60439, USA, ³Swiss Light Source, PSI, CH-5232 Villigen, Switzerland, ⁴Department of Physics, Technion, Haifa 32000, Israel, ⁵Laboratoire de Physique des Solides, Université Paris-Sud CNRS-UMR 8502, 91405 Orsay Cedex, France, ⁶Institute of Materials Science, University of Tsukuba, Ibaraki 305-3573, Japan, ⁷Physics Department, Brookhaven National Laboratory, PO Box 5000, Upton, New York 11973, USA, ⁸Max Planck Institute for Solid State Research, D-70569 Stuttgart, Germany, ⁹Department of Physics, The Ohio State University, Columbus, Ohio 43210, USA. *e-mail: jcc@uic.edu.

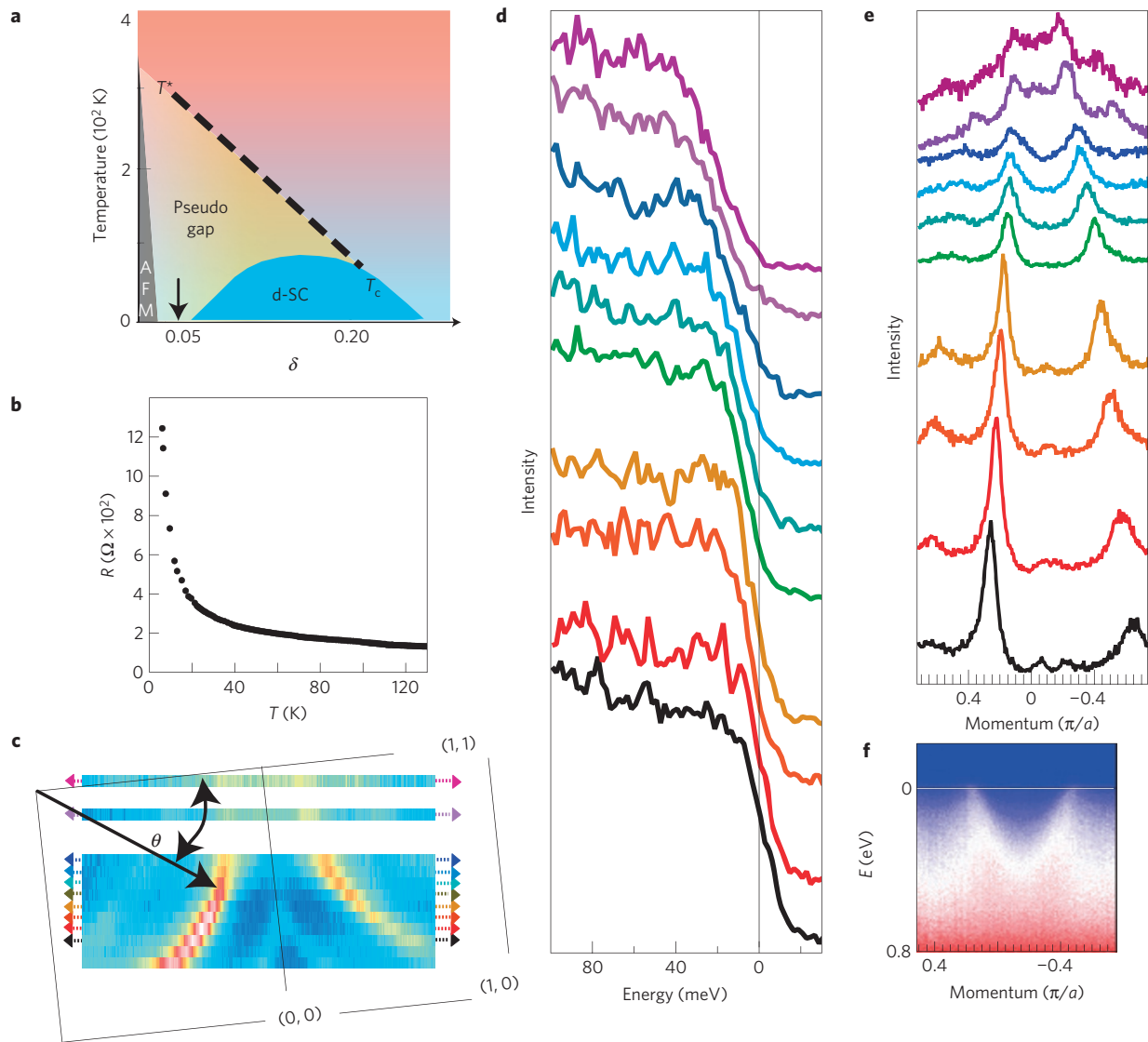


Figure 1 | Data for insulating samples. **a**, Phase diagram of $\text{Bi}_2\text{Sr}_2\text{CaCu}_2\text{O}_{8+\delta}$ in the hole-doping (δ), temperature (T) plane (the arrow indicates δ for the insulator) AFM: antiferromagnet. **b**, Resistance versus T . **c**, ARPES intensity versus \mathbf{k} at $T = 16$ K (averaged over a 0 to 10 meV window). The high-intensity points map out the underlying Fermi surface (\mathbf{k}_F) versus angle θ . **d**, EDCs at \mathbf{k}_F with θ increasing from 0° (top) to 45° (bottom). **e**, MDCs along the cuts marked in **c** (same colour coding in **c–e**). The top two MDCs are at $E = 18$ and 22 meV respectively; the rest are at $E = 0$ meV. **f**, Nodal dispersion for a $\delta = 0.04$ sample different from that in **c–e**.

In the insulator (Fig. 2d) we see a highly anisotropic energy gap that decreases monotonically from a maximal value at $\theta = 0^\circ$, to zero at $\theta = 45^\circ$. Even though there are no sharp coherence peaks at any angle, there is a clearly discernible low-energy gap. This is the pseudogap at low temperature (16 K) in the non-superconducting sample. With increasing doping, we move from the insulator (Fig. 2d) to the highly underdoped superconductor (Fig. 2e), for which the EDCs look qualitatively similar to those in Fig. 2d, except for the appearance of observable coherent quasiparticle peaks at the gap edge for all θ . These peaks grow in strength with increasing doping (Fig. 2f,g), as the energy gap evolves smoothly going from the insulator (Fig. 2d) to the optimally doped superconductor (Fig. 2e–g).

Much of the EDC intensities in Fig. 2d can be traced to a large ‘background’ that is present for all \mathbf{k} -points in the zone. The origin of this background is not entirely clear, although it can be readily identified as the ARPES spectra for unoccupied states (\mathbf{k} much beyond \mathbf{k}_F), or extracted from the ‘flat’ (\mathbf{k} -independent) part of the MDCs (ref. 8), and is plotted in Fig. 2b. We note that following the

signal, the intensity of the background also continuously decreases with decreasing doping (see Supplementary Information). If this background is subtracted from the data in Fig. 1d, we obtain the symmetrized results shown in Fig. 2c, which further emphasize the presence of a low-energy pseudogap ($\theta = 0^\circ$) and a node ($\theta = 45^\circ$).

Figure 3 shows the angular anisotropy of the spectral gap (Δ) for all of our thin-film and single-crystal samples. The superconducting samples were measured at temperatures between 16 and 40 K, well below their T_c ; the non-superconducting sample was measured at 16 K. The energy gap of the superconducting samples was determined from half the spacing between coherence peaks in symmetrized spectra at their corresponding \mathbf{k}_F . For the non-superconducting sample, we determine the low-energy gap from the raw data (as indicated by the intersection of red straight lines in Fig. 2d), from the background-subtracted data (Fig. 2c), and also from line-shape fits. All three methods lead to the same gap estimates within error bars.

Normalizing the gaps to their maximal value at $\theta = 0^\circ$, we find (Fig. 3a) that they follow a simple $|\cos(2\theta)|$ behaviour for all

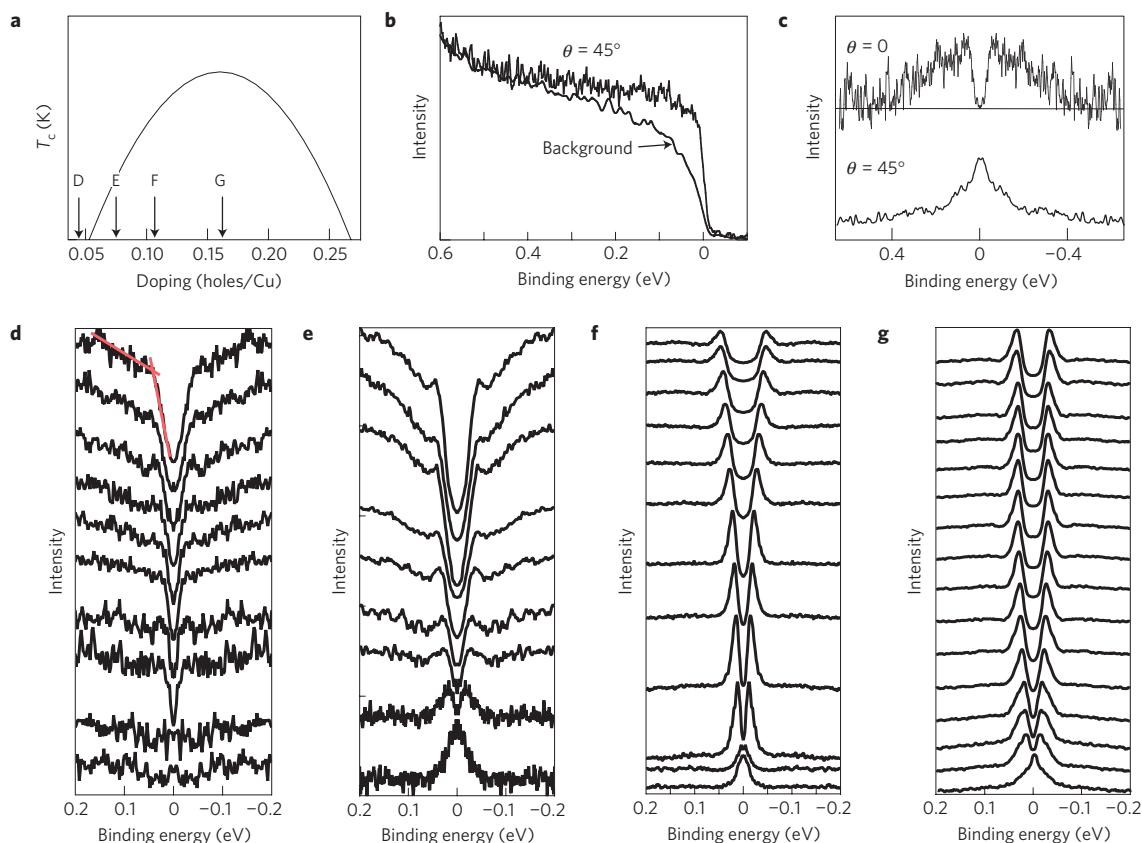


Figure 2 | Spectral function versus doping. **a**, Doping levels δ of four samples for which spectra are plotted in **d-g**. **b**, Insulator nodal spectrum and background (D in **a**) at $T = 16$ K. **c**, Background-subtracted, symmetrized intensity for sample D, showing a gap at the antinode and zero gap at the node. **d-g**, Symmetrized EDCs for an insulating film at $T = 16$ K (**d**), a $T_c = 33$ K film at $T = 16$ K (**e**), a $T_c = 69$ K crystal at $T = 20$ K (**f**) and a $T_c = 80$ K film at $T = 40$ K (**g**); the spectra are plotted from the antinode (top) to the node (bottom). The intersection of the red lines in **d** defines the gap in the insulator.

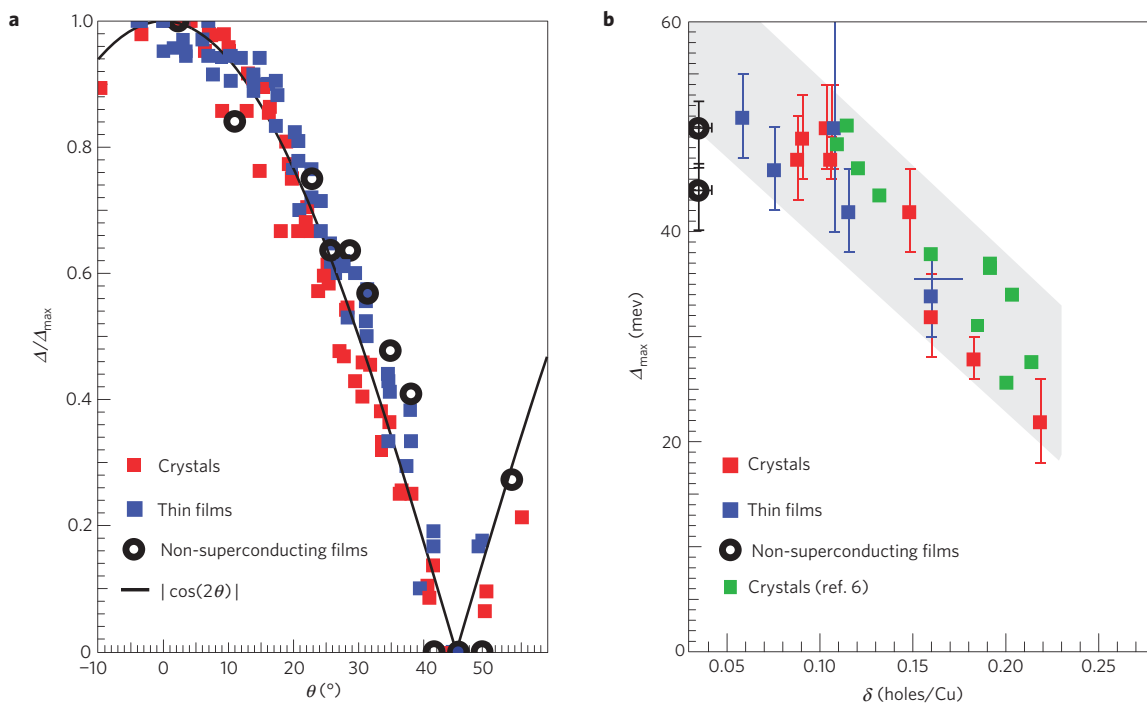


Figure 3 | The spectral gap as a function of doping and angle around the Fermi surface. **a**, The spectral gap $\Delta(\theta)$, normalized by its value at the antinode, versus the Fermi surface angle θ . $\Delta(\theta)$ at all doping levels is consistent with the d -wave form $|\cos(2\theta)|$ (black curve). **b**, Maximum gap as a function of hole-doping. Gaps of the superconducting samples are denoted by filled symbols (blue for thin films and red for single crystals, and green for published data⁶), and open circles are used for the non-superconducting samples. Error bars are given by the uncertainty in EDC peak positions at \mathbf{k}_F .

samples, superconducting and non-superconducting. This ‘ d -wave’ gap is universal in nature, and does not distinguish between the d -wave superconductor and the low-temperature pseudogap phase. The maximal energy gap values, plotted in Fig. 3b, monotonically increase with underdoping as found earlier⁶, although they might decrease near the superconductor–insulator boundary.

Our results confirm an earlier extrapolation⁹, based on ARPES measurements above T_c for underdoped superconducting samples, that the low-temperature pseudogap phase should be characterized by a node along the zone diagonal. They are also consistent with thermal conductivity (κ) measurements¹⁰ in highly underdoped $\text{YBa}_2\text{Cu}_3\text{O}_{6+\delta}$, which show that the low-temperature κ/T of the insulating phase proximate to the superconducting dome is the same as that in the d -wave superconducting phase, where it is dominated by nodal excitations.

Many experiments report a node in the superconducting state but a gap that deviates from the simple $|\cos(2\theta)|$ form with underdoping. This behaviour is attributed to two different order parameters (see ref. 11 and references therein), with an energy gap in the antinodal region (near $\theta = 0^\circ$) larger than what would be inferred by extrapolating the gap from the nodal region ($\theta = 45^\circ$). Our own work¹² a decade ago found evidence for a flattening of the gap around the nodes, but at that time the detectors had at least an order of magnitude lower \mathbf{k} -resolution and sparser angular sampling compared with the present study. Recent ARPES studies^{13–15} and scanning tunnelling microscopy^{16,17} have also reported ‘two gap’ behaviour.

The present results are not consistent with a two-gap picture. Several other experiments also find evidence for a simple d -wave gap. These include thermal transport data¹⁸, where the nodal-gap slope extrapolated to the antinode was consistent with the maximum gap, and ARPES data on underdoped $\text{La}_{2-x}\text{Sr}_x\text{CuO}_4$ (ref. 19), $1/8$ -doped $\text{La}_{2-x}\text{Ba}_x\text{CuO}_4$ (ref. 20) and $\text{Bi}2201$ (refs 21, 22). Why some experiments and/or samples show ‘two-gap’ behaviour whereas others show a simple d -wave gap is not understood at present. We must emphasize here that we observe coherent quasiparticle peaks at the gap edge at all \mathbf{k}_F for all superconducting samples down to the lowest T_c values. If, however, quasiparticle peaks were absent near the antinodes, one would erroneously estimate much larger gap values in the vicinity of these \mathbf{k} -points.

Another important question in highly underdoped samples is the possible existence of hole pockets, reported in a recent ARPES measurement²³. We have not found any evidence for such pockets. Our MDCs always trace out a large underlying Fermi surface as in Fig. 1c.

This brings us to the implications of our main result, the observation of a d -wave-like gap that persists through the insulator-to-superconductor transition. One possibility is that our insulating sample is highly inhomogeneous and has a small fraction of superconducting regions that dominate the low-energy signal, whereas the less-doped insulating regions produce the large spectroscopic background and dominate the transport. This inhomogeneity should be intrinsic, and not a surface phenomenon, because we have found very similar results in the superconducting samples for thin films and single crystals of $\text{Bi}_2\text{Sr}_2\text{CaCu}_2\text{O}_{8+\delta}$, as well as single crystals of $\text{La}_{2-x}\text{Sr}_x\text{CuO}_4$ (ref. 19) (which involved a completely different surface preparation). We emphasize that our diamagnetic susceptibility measurement puts a bound of 1% on the superconducting fraction, which seems too small to account for the signal-to-background ratio observed in Fig. 2b. The $T = 0$ superconductor-to-insulator transition is driven by quantum fluctuations²⁴ of the phase of the superconducting order parameter. The corresponding thermal fluctuations, which are vortex-like excitations in the pseudogap phase, have been probed by Nernst²⁵ and diamagnetism²⁶ experiments.

Our observations imply that the sharp quasiparticles of the superconducting state exist down to the lowest doping levels while rapidly losing spectral weight, but are no longer visible on the insulating side. Nonetheless, a low-energy d -wave-like gap survives the phase-disordering transition. Obviously, the node must disappear as the Mott insulator is approached²⁷. We note that sample charging prevents us from making low-temperature measurements for $\delta < 0.04$, suggesting a fully gapped insulator.

We emphasize that our experiments probe the excitation spectrum, but not any possible broken symmetries of the nodal-liquid state. The simplest picture consistent with our data is that the nodal liquid is just a phase-incoherent version of the d -wave superconductor^{28–30}, and adding charged carriers to this liquid establishes phase coherence, leading to high- T_c superconductivity.

Received 13 August 2009; accepted 22 October 2009;
published online 22 November 2009

References

- Kastner, M. A. & Birgenau, R. J. Magnetic, transport, and optical properties of monolayer copper oxides. *Rev. Mod. Phys.* **70**, 897–928 (1998).
- Tsuei, C. C. *et al.* Robust $d_{x^2-y^2}$ pairing symmetry in hole-doped cuprate superconductors. *Phys. Rev. Lett.* **93**, 187004 (2004).
- Konstantinovic, Z., Li, Z. Z. & Raffy, H. Normal state transport properties of single- and double-layered $\text{Bi}_2\text{Sr}_2\text{Ca}_{n-1}\text{Cu}_n\text{O}_y$ thin films and the pseudogap effect. *Physica C* **341–348**, 859–862 (2000).
- Oh, S., Crane, T. A., Van Harlingen, D. J. & Eckstein, J. N. Doping controlled superconductor–insulator transition in $\text{Bi}_2\text{Sr}_2\text{La}_x\text{CaCu}_2\text{O}_{8-\delta}$. *Phys. Rev. Lett.* **96**, 107003 (2006).
- Matei, I., Li, Z. Z. & Raffy, H. Observation of the superconducting–insulating transition in a $\text{BiSr}(\text{La})\text{CuO}$ thin film tuned by varying the oxygen content. *J. Phys.: Conf. Ser.* **150**, 052154 (2009).
- Campuzano, J. C. *et al.* Electronic spectra and their relation to the (π, π) collective mode in high- T_c superconductors. *Phys. Rev. Lett.* **83**, 3709–3712 (1999).
- Norman, M. R. *et al.* Destruction of the Fermi surface in underdoped high- T_c superconductors. *Nature* **392**, 157–160 (1998).
- Kaminski, A. *et al.* Identifying the background signal in angle-resolved photoemission spectra of high-temperature cuprate superconductors. *Phys. Rev. B* **69**, 212509 (2004).
- Kanigel, A. *et al.* Evolution of the pseudogap from Fermi arcs to the nodal liquid. *Nature Phys.* **2**, 447–451 (2006).
- Doiron-Leyraud, N. *et al.* Onset of a Boson mode at the superconducting critical point of underdoped $\text{YBa}_2\text{Cu}_3\text{O}_x$. *Phys. Rev. Lett.* **97**, 207001 (2006).
- Huefner, S., Hossain, M. A., Damascelli, A. & Sawatzky, G. A. Two gaps make a high-temperature superconductor? *Rep. Prog. Phys.* **71**, 062501 (2008).
- Mesot, J. *et al.* Superconducting gap anisotropy and quasiparticle interactions: A doping dependent photoemission study. *Phys. Rev. Lett.* **83**, 840–843 (1999).
- Tanaka, K. *et al.* Distinct Fermi-momentum-dependent energy gaps in deeply underdoped $\text{Bi}2212$. *Science* **314**, 1910–1913 (2006).
- Ma, J.-H. *et al.* Coexistence of competing orders with two energy gaps in real and momentum space in the high temperature superconductor $\text{Bi}_2\text{Sr}_{2-x}\text{La}_x\text{CuO}_{6+\delta}$. *Phys. Rev. Lett.* **101**, 207002 (2008).
- He, R.-H. *et al.* Energy gaps in the failed high- T_c superconductor $\text{La}_{1.875}\text{Ba}_{0.125}\text{CuO}_4$. *Nature Phys.* **5**, 119–123 (2009).
- Pushp, A. *et al.* Extending universal nodal excitations optimizes superconductivity in $\text{Bi}_2\text{Sr}_2\text{CaCu}_2\text{O}_{8+\delta}$. *Science* **324**, 1689–1693 (2009).
- Lee, J. *et al.* Spectroscopic fingerprint of phase incoherent superconductivity in the pseudogap state of underdoped $\text{Bi}_2\text{Sr}_2\text{CaCu}_2\text{O}_{8+\delta}$. *Science* **325**, 1099–1103 (2009).
- Sutherland, M. *et al.* Thermal conductivity across the phase diagram of cuprates: Low-energy quasiparticles and doping dependence of the superconducting gap. *Phys. Rev. B* **67**, 174520 (2003).
- Shi, M. *et al.* Coherent d -wave superconducting gap in underdoped $\text{La}_{2-x}\text{Sr}_x\text{CuO}_4$ by angle-resolved photoemission spectroscopy. *Phys. Rev. Lett.* **101**, 047002 (2008).
- Valla, T. *et al.* The ground state of the pseudogap in cuprate superconductors. *Science* **314**, 1914–1916 (2006).
- Meng, J. *et al.* Monotonic d -wave superconducting gap of the optimally doped $\text{Bi}_2\text{Sr}_{1.6}\text{La}_{0.4}\text{CuO}_6$ superconductor by laser-based angle-resolved photoemission spectroscopy. *Phys. Rev. B* **79**, 024514 (2009).
- Wei, J. *et al.* Superconducting coherence peak in the electronic excitations of a single-layer $\text{Bi}_2\text{Sr}_{1.6}\text{La}_{0.4}\text{CuO}_{6+\delta}$ cuprate superconductor. *Phys. Rev. Lett.* **101**, 097005 (2008).

23. Meng, J. *et al.* Direct observation of Fermi pocket in high temperature cuprate superconductors. Preprint at <<http://arxiv.org/abs/0906.2682>> (2009).
24. Hetel, I., Lemberger, T. R. & Randeria, M. Quantum critical behaviour in the superfluid density of strongly underdoped ultrathin copper oxide films. *Nature Phys.* **3**, 700–702 (2007).
25. Wang, Y., Li, L. & Ong, N. P. Nernst effect in high- T_c superconductors. *Phys. Rev. B* **73**, 024510 (2006).
26. Li, L., Chechelsky, J. G., Komiya, S., Ando, Y. & Ong, N. P. Low-temperature vortex liquid in $\text{La}_{2-x}\text{Sr}_x\text{CuO}_4$. *Nature Phys.* **3**, 311–314 (2007).
27. Shen, K. M. *et al.* Fully gapped single-particle excitations in lightly doped cuprates. *Phys. Rev. B* **69**, 054503 (2004).
28. Anderson, P. W. *et al.* The physics behind high-temperature superconducting cuprates: The ‘plain vanilla’ version of RVB. *J. Phys. Condens. Mater.* **16**, R755–R799 (2004).
29. Balents, L., Fisher, M. P. A. & Nayak, C. Nodal liquid theory of the pseudo-gap phase of high- T_c superconductors. *Int. J. Mod. Phys. B* **12**, 1033–1068 (1998).
30. Tesanovic, Z. *d*-wave duality and its reflections in high-temperature superconductors. *Nature Phys.* **4**, 408–414 (2008).

Acknowledgements

Work supported by the US National Science Foundation under grant DMR-0606255 (J.C.C.), NSF-DMR 0706203 (M.R.), and the US Department of Energy, Office of Science, under contract Nos DE-AC02-06CH11357 and DE-AC02-98CH10886. The Synchrotron Radiation Center, University of Wisconsin-Madison, is supported by the National Science Foundation under Award No. DMR-0537588.

Author contributions

Project planning: J.C.C.; sample preparation: H.R., Z.Z.L., K.K., D.G.H., Z.J.X., J.S.W., G.G. and C.T.L.; ARPES experiments: U.C., M.S., D.A., J.Z., A.K. and S.R.; resistivity measurements: H.R. and Z.Z.L.; susceptibility measurements: H.C.; data analysis: U.C., M.S., D.A., A.K., M.R.N. and J.C.C.; manuscript preparation: U.C., M.R.N., M.R. and J.C.C.

Additional information

Supplementary information accompanies this paper on www.nature.com/naturephysics. Reprints and permissions information is available online at <http://npg.nature.com/reprintsandpermissions>. Correspondence and requests for materials should be addressed to J.C.C.